IEEE VTS Motor Vehicles Challenge 2024 - Energy and Powertrain Losses Management of an e-Racing Vehicle

Ke Li
Power Electronics, Machines and Control (PEMC) group
Faculty of Engineering
University of Nottingham
Nottingham, UK
ke.li2@nottingham.ac.uk

Thanh Vo-Duy*
CTI Lab. for EVs
School of Electrical and Electronic Engineering
Hanoi University of Science and Technology
Hanoi, Vietnam
thanh.voduy@hust.edu.vn

***Abstract*—Motor Vehicle Challenge, supported by IEEE Vehicular Technology Society, is an annual activity to find an appropriate energy management strategy to improve electric vehicles' performance. In Challenge 2024, power losses and efficiency of power converters using silicon carbide MOSFET and an internal permanent magnet (IPM) motor are modelled and implemented into an electric vehicle powertrain model for a racing vehicle with hybrid energy storage sources. The objective of the developed energy management strategy is to minimise both the size, energy consumption of the energy storage sources and the losses and cost of all the power electronics converters. Participants from both academia and industry are welcome to participate and submit the solutions for the Challenge.**

***Index Terms*—Energy management, power electronics converters, electric machines, silicon carbide MOSFET, efficiency**

I. Introduction

To fight against global warming and to reduce CO2 emission of road transportation, the numbers of the electric vehicles (EVs) have been growing in an exponential way recently. Despite the improvement in driving range and the overall performance in the last decade, there are still concerns over EVs' limited battery life, charging infrastructures, higher cost and overall efficiency. To address these issues, battery management, hybrid energy storage components managements, reliable and more efficient power electronics converter and electric machines are all the important research areas to bring a step change for EVs' performance in comparison with today's technology.

With the purpose to attract more researchers and engineers to improve EVs' performance, an annual Motor Vehicle Challenge (MVC) was launched in IEEE VPPC 2016 and the Challenge was supported by IEEE Vehicular Technology Society (VTS). In previous editions of the MVC, the participants were invited to propose an energy management strategy (EMS) to reduce operation cost of an hybrid vehicle [1], its fuel consumption and the battery recharging cost [2], hydrogen consumption of a dual-mode locomotive [3] and heavy-duty track [4], battery state-of-charge of a dual-motor all-wheel drive [5], and sizing of a commercial EV with hybrid dual-energy storage systems [6].

In addition to an effective energy management strategy to improve EVs' performance, the efficiency of the power electronics converters and electric machines play an equally important role to extend the range and reduce the overall system cost [7], [8]. We note that in previous editions of the MVC, the used simulation model for power electronics converters and electric machines are quite simple, which do not represent their real power losses and efficiency over an entire driving cycle. To address the issue, in MVC2024, we will propose a simulation model that take into consideration of the losses and efficiency of the power electronics converters and electric machines. Therefore, the developed EMS will produce simulation results more close to the real applications than using a simple model, and it would be interesting to know whether the previous winning EMS were still the best options.

In this paper, we will provide an EV model of a racing vehicle from the University of Nottingham, and we will add additional models of power losses and efficiency of power converters and electric machine. The participant are required to develop an appropriate EMS not only to minimise the size and to extend the battery life, but also to reduce the overall losses and cost of power converters and electric machine.

The paper is structured with following sections. Section II describes the studied EV powertrain model. Section III presents the loss model of the power electronics converters and the electric machine. Following that, the requirement of the EMS is described with more details in Section IV. The paper is concluded finally in Section V.

II. Electric vehicle powertrain model

The configuration of the studied EV as the platform of the challenge is illustrated in Fig. 1. This platform is based on a racing vehicle from the University of Nottingham whose energy storage system is modified by the addition of a super capacitor pack and two bi-directional DC/DC converters. This configuration forms a hybrid energy storage system (HESS)

(a) Photo

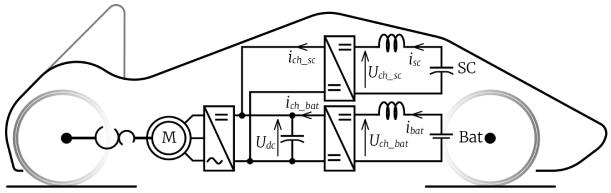

(b) Configuration

Fig. 1: Photo and configuration of the studied EV

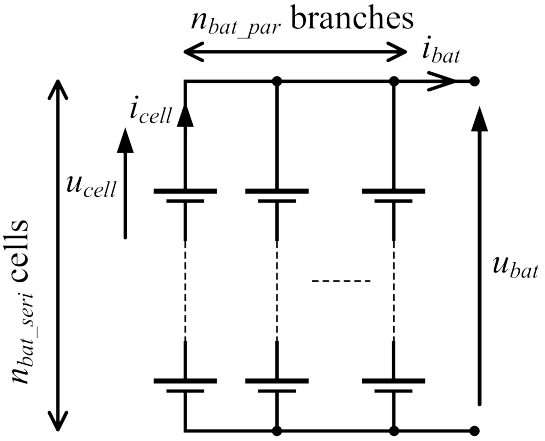

Fig. 2: Connection in battery system

that need to be managed optimally to extend the battery life-span and/or racing distance.

The HESS energizes an internal permanent magnet (IPM) motor through an inverter. This traction motor is connected to a gearbox to drive the rear wheel of the EV. In this paper, losses of all power electronic converters as well as of the traction motor are taken into account when the vehicle runs.

A. Energy storage components model

1) Modeling of battery system: The battery system consists of numbers of cells that are connected in series and parallel as described in Fig. 2. Each cell is modeled by its equivalent circuit as follows.

$$\begin{cases} u_{cell} = u_{OCV}(\text{SoC}) - i_{cell} R_{int} \\ \text{SoC} = 1 - \dfrac{1}{3600 Q_{rated}} \int i_{cell} dt \end{cases} \tag{1}$$

where, u_{cell} and i_{cell} are voltage and current of each cell, respectively. R_{int} is the internal resistance of battery cell, Q_{rated} denotes the cell capacity. In the model (1), the open circuit voltage u_{OCV} is a function of the state-of-charge of the battery cell which is provided by an experimental characteristic.

The relationship of the output voltage u_{bat} and current i_{bat} of the whole battery pack and those of each cell can be described by (2).

$$\begin{cases} u_{bat} = n_{bat\_seri} u_{cell} \\ i_{cell} = \dfrac{1}{n_{bat\_par}} i_{bat} \end{cases} \tag{2}$$

2) Modeling of super capacitor system: Super capacitor (SC) system contains various cell/module as well. In this challenge, a simple model (3) of SC is used.

$$u_{sc} = u_{sc\_0} - R_{esr} i_{sc} - \frac{1}{C_{rated}} \int i_{sc} dt \tag{3}$$

where, u_{sc} and u_{sc_0} are the output voltage and the initial voltage of the whole SC pack, respectively. R_{esr} denotes the equivalent series resistor, C_{rated} is the capacitance of the SC pack. i_{sc} is the current, going in or out of the pack.

B. Power electronics converter model

As illustrated in Fig. 1b, two DC-DC bi-directional power converters are used to connect between each energy storage source and the DC bus. For battery converter, the voltage and current are modelled by following equations (the SC converter follows the same form):

$$\begin{cases} u_{ch\_bat} = m_{bat} u_{dc} \\ i_{ch\_bat} = m_{bat} i_{bat} \eta^{-k} \end{cases} \tag{4}$$

where m_{bat} is the duty cycle, η is the efficiency and k is a parameter represents the direction of the current i_{bat}. $k = 1$ when $i_{\text{bat}} < 0$ and $k = -1$ when $i_{\text{bat}} > 0$.

C. Electric machine model

The model of the traction IPM motor is developed on d-q frame which includes three parts, i.e., electric, electro-mechanic, and mechanic models [9].

The electric equations of the IPM motor includes models of the armature and the field which are the relationship between input voltages in d-q frame U_d, U_q and motor currents I_d, I_q.

$$\begin{aligned} I_d &= (U_d - E_d) \frac{1}{L_d s + R_s} \\ I_q &= (U_q - E_q) \frac{1}{L_q s + R_s} \end{aligned} \tag{5}$$

where, L_d, L_q and R_s are inductance on d, q axes and resistance of motor winding, respectively. E_d and E_q denote

Fig. 3: Commercial 1200V/100A SiC-MOSFET power module [11]

the back electromotive force (EMF) which are obtained from electro-mechanic model as follows.

$$T_e = \frac{3p}{2}[\phi_{pm} I_q + (L_d - L_q) I_d I_q] \tag{6}$$

$$\begin{aligned} E_d &= -L_q I_q \omega_e \\ E_q &= L_d I_d \omega_e + \phi_{pm} \omega_e \end{aligned} \tag{7}$$

where, T_e is the motor torque at its shaft, ϕ_{pm} is the flux of the permanent magnet, ω_e is the synchronous speed which is calculated from the number of pole pair p and the rotor speed Ω_m, i.e., $\omega_e = p\Omega_m$.

The mechanical model of the IPM motor is written as follows.

$$T_e - T_{load} = J\frac{d\Omega_m}{dt} \tag{8}$$

in which, T_{load} is the load torque, and J is the moment of inertia of the motor. In EV applications, the load torque is all resistance in the system that is converted to the shaft of the motor, for example, air and rolling resistance force.

III. Power Electronics Converter and Electric Machine Losses Model

A. Silicon carbide power module

With the superior characteristics to operate at higher power, efficiency and temperature than silicon power semiconductor devices, silicon carbide (SiC) power transistors and modules are becoming more and more popular to be applied in EV-based power electronics converters [10].

We will use a 1200V/100A SiC-MOSFET module (CAB011M12FM3) [11] for this challenge, which is shown in Fig. 3. The module is in half-bridge layout, with one MOSFET located at upper side and another one located at lower side. As MOSFET has a body-diode, the current can flow through each MOSFET in bi-direction.

Power losses of a SiC-MOSFET can be divided into both conduction losses and switching losses. Dependent on the current direction, the losses of each MOSFET is different and will be analysed below.

B. Power converter losses mechanism

A half-bridge layout is presented in Fig. 4, where the control signals of the two MOSFETs of one switching cycle are complementary to each other. Between 0-t_1 and t_2-t_3, the lower device S_2 is in conduction, and we need to count device

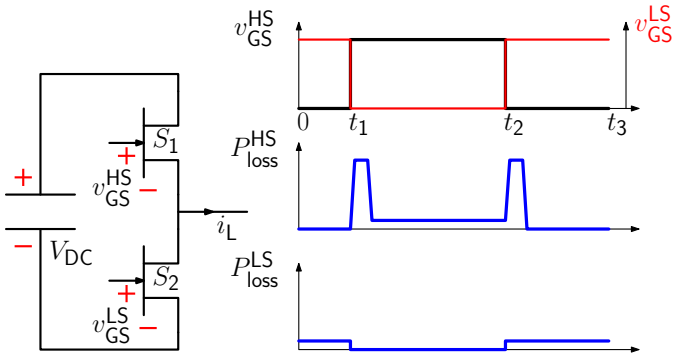

Fig. 4: Loss mechanism of a half-bridge layout

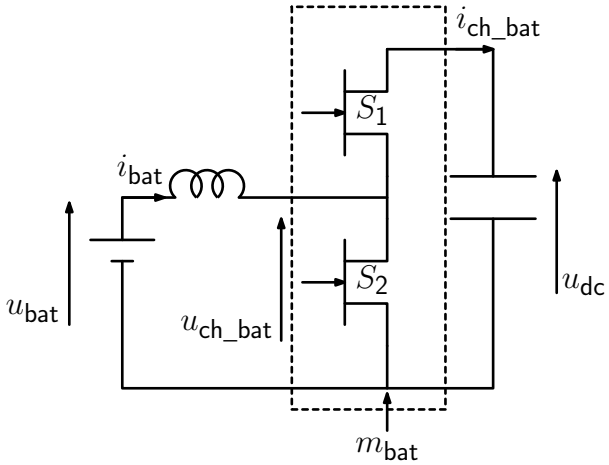

Fig. 5: Modelling power converter losses used in the EV powertrain

conduction losses. By contrast, between t_1-t_2, we need to count conduction losses P_{cond} of upper device S_1. When the current is superior to 0 under the direction illustrated in the figure, there are switching losses P_{sw} of S_1 at instant t_1 and t_2 because current and voltage of S_1 are in the same sign. As current and voltage of S_2 are in opposite sign, the switching losses of S_2 can be neglected. Therefore, for MOSFET S_1, the average power losses P_{loss}^{HS} of one switching cycle is:

$$P_{\text{loss}}^{HS} = P_{\text{cond}} \cdot m + E_{\text{sw}} \cdot f_{\text{sw}} \tag{9}$$

For MOSFET S_2, the average power losses P_{loss}^{LS} of one switching cycle is:

$$P_{\text{loss}}^{LS} = P_{\text{cond}} \cdot (1 - m) \tag{10}$$

In the above equations, m is the duty cycle of MOSFET S_1, E_{sw} is the switching energy and f_{sw} is the switching frequency.

When the current direction is inferior to 0, we need to only consider P_{cond} for upper device, but both P_{cond} and P_{sw} for lower device.

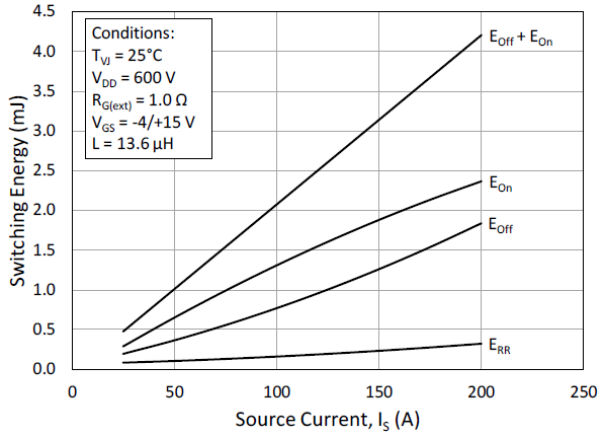

(a) Dependency of E_{sw} with switching current

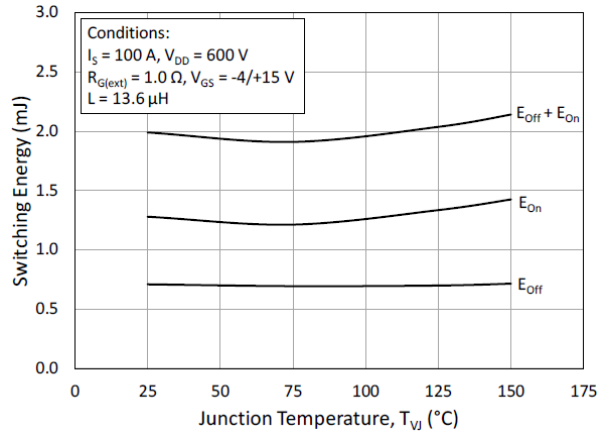

(b) Dependency of E_{sw} with temperature

Fig. 6: Dependency of E_{sw} with switching current and temperature [11]

TABLE I: Power losses of each transistor used in the EV powertrain

	$i_{\text{bat}} > 0$	$i_{\text{bat}} < 0$
P_{loss}^{LS} of S_2	P_{cond}(1-m_{bat})+P_{sw}	P_{cond}(1-m_{bat})
P_{loss}^{HS} of S_1	$P_{\text{cond}} m_{\text{bat}}$	$P_{\text{cond}} m_{\text{bat}}$+$P_{\text{sw}}$

C. Power converter losses model

The presented DC-DC converter can be replaced by the above half-bridge circuit. The equivalent circuit is then given in Fig. 5. The power losses of each transistor can be summarised in TABLE I depending on the direction of the battery current i_{bat}.

Both eq.(9) (10) can be used to calculate transistor losses.

$$P_{\text{cond}} = i_{\text{bat}}^2 \cdot R_{\text{on}} \tag{11}$$

Where R_{on} is the ON-state resistance of the MOSFET, and its dependency with the temperature is not considered here.

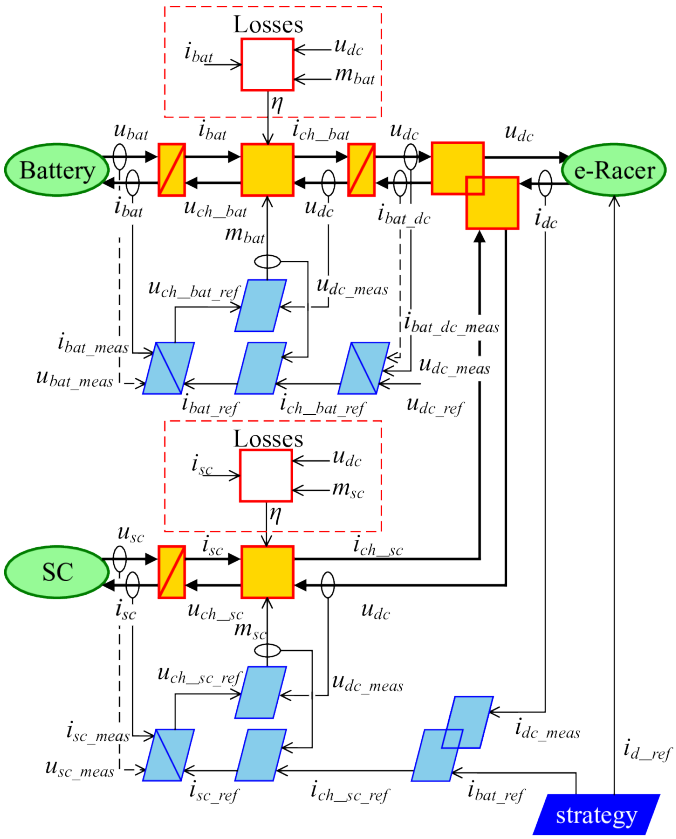

Fig. 7: Powertrain system representation including power converter losses

Regarding switching energy E_{sw}, it is mainly dependent on the switching current rather than the temperature (Fig. 6). The current dependency can be modelled by a linear function.

$$E_{\text{sw}} = a_{\text{sw}} i_{\text{bat}} + b_{\text{sw}} \tag{12}$$

Finally, T_{j} of each MOSFET can be obtained by the thermal equation:

$$T_{\text{j}} - T_{\text{amb}} = P_{\text{loss}}^{x} \cdot R_{\text{th}} \tag{13}$$

where x represents either HS or LS MOSFET, T_{amb} is ambient temperature of 20°C and R_{th} is junction to heatsink thermal resistance of $0.5°C/W$.

Therefore, the total losses of the power converter is:

$$P_{\text{loss}} = P_{\text{loss}}^{LS} + P_{\text{loss}}^{HS} \tag{14}$$

And the efficiency of the power converter can be obtained as:

$$\eta = \frac{i_{\text{bat}} \cdot u_{\text{dc}} \cdot m_{\text{bat}} - P_{\text{loss}}}{i_{\text{bat}} \cdot u_{\text{dc}} \cdot m_{\text{bat}}} \tag{15}$$

The implementation of the presented power converter loss and efficiency model for both battery and SC DC-DC converters is shown in Fig. 7, where the losses and efficiency can be simulated and obtained together with the powertrain

system control model. For battery converter, the input to the subsystem for loss and efficiency simulation is i_{bat}, u_{dc} and m_{bat}, and the output of the subsystem is total power losses and the efficiency η. The efficiency will be fed back to the DC/DC converter model to compute the current $i_{\mathrm{ch\_bat}}$.

The same loss and efficiency model is also implemented for SC DC-DC converter and for the inverter, therefore the loss and efficiency can be obtained with the whole powertrain control model.

D. Electric machine losses model

The motor loss is mainly caused by materials of the motor, in which, iron loss P_{fe} in the core and copper loss P_{cu} in the stator coil are dominant. The iron loss consists of hysteresis and eddy current losses which happen when working in alternating field. Besides, there are also losses caused by higher winding space and slot harmonics that is called stray loss P_{str}. The total motor loss P_{tot} in this paper is written as follows [12].

$$\begin{aligned} P_{tot} &= P_{cu} + P_{fe} + P_{str} \\ &= \frac{3}{2} R_s (I_d^2 + I_q^2) + c_{fe} \omega_e^{\gamma} (\lambda_d^2 + \lambda_q^2) + c_{str} \omega_e^2 (I_d^2 + I_q^2) \end{aligned} \tag{16}$$

where, $\lambda_d = L_d I_d + \phi_{pm}$ and $\lambda_q = L_q I_q$ are the motor flux on the d- and q-axis. c_{fe}, c_{str} are iron loss and stray loss coefficients, respectively. γ is chosen of 1.6.

IV. Energy and Powertrain Losses Management

As illustrated in Fig. 7, we will use the approach of energetic macroscopic representation (EMR) for the control of the powertrain [13], as EMR has been widely applied for energy management and control of complex electro-mechanic systems such as electric vehicle [14], [15], railway [16], subway [17], [18], and renewable energy systems [19].

A. Objective

The objective of the MVC is to propose a strategy to deal with the two degrees of the freedom ($I_{\mathrm{bat\_ref}}$ and $I_{\mathrm{d\_ref}}$ in Fig. 7), which is able to minimise the size, energy consumption of the energy storage components as well as the losses of the powertrain (power converters and electric machine) and the cost (the numbers of the SiC-MOSFET modules) over a provided driving cycle (one example is given in Fig. 8).

An objective function is defined as

$$J = k_1 \Delta\mathrm{SoC} + k_2 |\Delta u_{\mathrm{sc}}| + k_3 \sigma_{\mathrm{cell}} + k_4 E_{regen} + k_5 P_{\mathrm{loss}}^{tot} + k_6 N \tag{17}$$

where k_{n} is a weighting factor.

ΔSoC shows the energy of the battery consumed for the EV to travel throughout a given driving cycle.

σ_{cell} is the standard deviation of each battery cell current which is obtained by (18)

$$\sigma_{cell} = \sqrt{\frac{\sum_{i=1}^{N} (i_{cell}(i) - \mu)^2}{N_{cell}}} \tag{18}$$

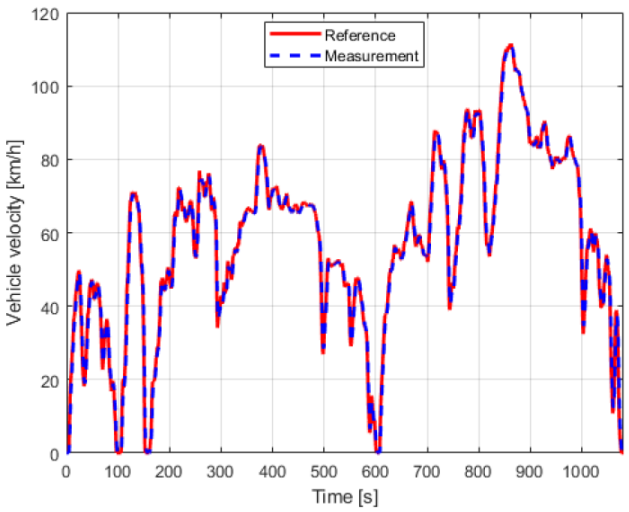

Fig. 8: A driving cycle used in simulation

with μ is the value that is calculated as follows

$$\mu = \frac{\sum_{i=1}^{N} i_{cell}(i)}{N} \tag{19}$$

E_{regen} is the regenerative energy to the battery when deceleration/braking.

$$E_{regen} = \int_0^t u_{bat} i_{bat} d\tau \Big|_{i_{bat}<0} \tag{20}$$

P_{loss}^{tot} is the total losses of battery DC-DC converter, supercapacitor DC-DC converter, the inverter and the traction motor.

N is the number of the needed SiC-MOSFET modules to satisfy the constraint of the maximal junction temperature $T_{\mathrm{j,max}}$ (175°C). $T_{\mathrm{j,max}}$ cannot be exceeded in simulation, otherwise N should be increased to reduce the power losses by $\frac{P_{\mathrm{loss}}^{tot}}{N}$.

The winning team will be selected to achieve a minimised value of J and to satisfy the T_{j} constraints among all the competition teams.

B. Case study

One case study of the obtained power losses and T_{j} of the battery DC-DC converter over one driving cycle under a chosen EMS is presented in Fig. 9, where one SiC-MOSFET power module is used. It should be noted that to increase simulation speed, we only include thermal resistance R_{th} in the simulation (thermal capacitance C_{th} is not considered). For S_2, the peak T_{j} is inferior to $T_{\mathrm{j,max}}$. However, for S_1, the peak T_{j} is superior to $T_{\mathrm{j,max}}$, which does not satisfy the constraint. To resolve it, at least two SiC-MOSFET power module should be used in parallel to reduce the power losses of each module if the same EMS is applied, or another EMS should be proposed to reduce peak T_{j} value.

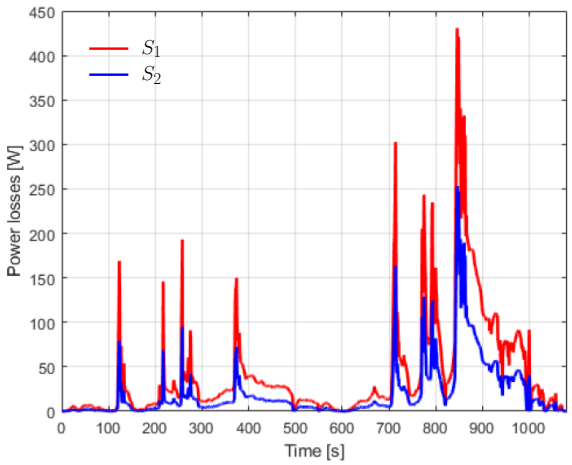

(a) Power losses

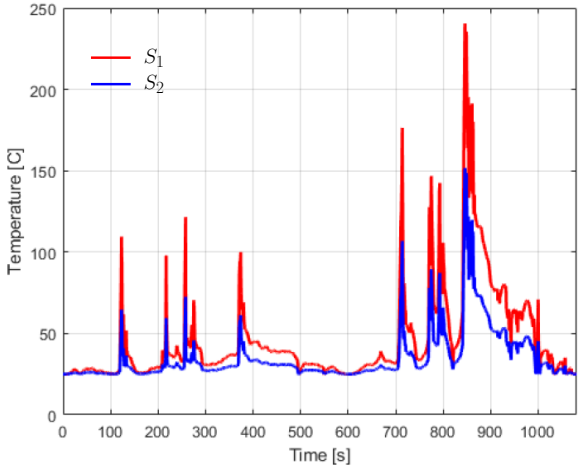

(b) T_{j}

Fig. 9: Obtained power losses and T_{j} of the battery DC-DC converter over one driving cycle

V. Conclusion

In this paper, it is presented a powertrain model for a racing vehicle. In comparison with the previously used powertrain models in Motor Vehicle Challenge, the losses and efficiency of the power converters and electric machine are considered in the model. A 1200V/100A SiC-MOSFET half-bridge power module is selected in the Challenge, and its power losses and efficiency are implemented into the powertrain model. In order to win the challenge, the participants are required to develop an appropriate strategy to minimise both the size, energy consumption of the energy storage components and the losses and cost of all the power electronics converters and electric machine. As power converter and electric machine real losses are considered in the simulation model, it will produce results more close to the real applications, which could eventually improve the design accuracy.

Acknowledgement

We would like to thank IEEE VTS and Motor Vehicle Challenge Committee for the support of the Challenge.

References

[1] C. Depature, S. Jemei, L. Boulon, A. Bouscayrol, N. Marx, S. Morando, and A. Castaings, "Ieee vts motor vehicles challenge 2017 - energy management of a fuel cell/battery vehicle," in *2016 IEEE Vehicle Power and Propulsion Conference (VPPC)*, pp. 1–6, 2016.

[2] C. Depature, S. Pagerit, L. Boulon, S. Jemei, A. Rousseau, and A. Bouscayrol, "Ieee vts motor vehicles challenge 2018 - energy management of a range extender electric vehicle," in *2017 IEEE Vehicle Power and Propulsion Conference (VPPC)*, pp. 1–6, 2017.

[3] W. Lhomme, T. Letrouve, L. Boulon, S. Jemei, A. Bouscayrol, F. Chauvet, and F. Tournez, "Ieee vts motor vehicles challenge 2019 - energy management of a dual-mode locomotive," in *2018 IEEE Vehicle Power and Propulsion Conference (VPPC)*, pp. 1–6, 2018.

[4] J. Solano, S. Jemei, L. Boulon, L. Silva, D. Hissel, and M.-C. Pera, "Ieee vts motor vehicles challenge 2020 - energy management of a fuel cell/ultracapacitor/lead-acid battery hybrid electric vehicle," in *2019 IEEE Vehicle Power and Propulsion Conference (VPPC)*, pp. 1–6, 2019.

[5] B.-H. Bao-Huy Nguyen, J. P. F. Trovao, S. Jemei, L. Boulon, and A. Bouscayrol, "Ieee vts motor vehicles challenge 2021 - energy management of a dual-motor all-wheel drive electric vehicle," in *2020 IEEE Vehicle Power and Propulsion Conference (VPPC)*, pp. 1–6, 2020.

[6] T. Vo-Duy, J. P. F. Trovao, S. Jemei, L. Boulon, M. C. Ta, and A. Bouscayrol, "Ieee vts motor vehicles challenge 2022 - sizing and energy management of hybrid dual-energy storage system for a commercial electric vehicle," in *2021 IEEE Vehicle Power and Propulsion Conference (VPPC)*, pp. 1–6, 2021.

[7] K. Li, P. Evans, and M. Johnson, "SiC/GaN power semiconductor devices: a theoretical comparison and experimental evaluation under different switching conditions," *IET Electrical Systems in Transportation*, vol. 8, no. 1, pp. 3–11, 2018.

[8] C. Liu, K. T. Chau, C. H. T. Lee, and Z. Song, "A critical review of advanced electric machines and control strategies for electric vehicles," *Proceedings of the IEEE*, vol. 109, no. 6, pp. 1004–1028, 2021.

[9] T. Vo-Duy and M. C. Ta, "Fundamental design of electric motor control systems," in *Encyclopedia of Electrical and Electronic Power Engineering* (J. García, ed.), pp. 428–453, Oxford: Elsevier, 2023.

[10] T. Do Van Thang, J. P. F. Trovao, K. Li, and L. Boulon, "Wide-Bandgap Power Semiconductors for Electric Vehicle Systems: Challenges and Trends," *IEEE Vehicular Technology Magazine*, pp. 2–11, 2021.

[11] Wolfspeed, "CAB011M12FM3 Datasheet."

[12] K. H. Nam, *AC Motor Control and Electrical Vehicle Applications*. Taylor & Francis, 2nd ed., 2019.

[13] A. Bouscayrol, X. Guillaud, P. Delarue, and B. Lemaire-Semail, "Energetic macroscopic representation and inversion-based control illustrated on a wind-energy-conversion system using hardware-in-the-loop simulation," *IEEE Transactions on Industrial Electronics*, vol. 56, no. 12, pp. 4826–4835, 2009.

[14] A. Jacome, C. Dépature, L. Boulon, and J. Solano, "A benchmark of different starting modes of a passive fuel cell/ultracapacitor hybrid source for an electric vehicle application," *Journal of Energy Storage*, vol. 35, p. 102280, 2021.

[15] H.-L. T. Nguyen, B.-H. Nguyen, T. Vo-Duy, and J. P. F. Trovao, "A comparative study of adaptive filtering strategies for hybrid energy storage systems in electric vehicles," *Energies*, vol. 14, no. 12, 2021.

[16] D. Ramsey, T. Letrouve, A. Bouscayrol, and P. Delarue, "Comparison of energy recovery solutions on a suburban dc railway system," *IEEE Transactions on Transportation Electrification*, vol. 7, no. 3, pp. 1849–1857, 2021.

[17] C. Mayet, P. Delarue, A. Bouscayrol, E. Chattot, and J.-N. Verhille, "Comparison of different emr-based models of traction power substations for energetic studies of subway lines," *IEEE Transactions on Vehicular Technology*, vol. 65, no. 3, pp. 1021–1029, 2016.

[18] C. Mayet, P. Delarue, A. Bouscayrol, and E. Chattot, "Emr-based simulation tool of a multi-train subway system," in *2016 IEEE Vehicle Power and Propulsion Conference (VPPC)*, pp. 1–6, 2016.

[19] K. S. Agbli, D. Hissel, M.-C. Péra, and I. Doumbia, "Emr modelling of a hydrogen-based electrical energy storage," *The European Physical Journal - Applied Physics*, vol. 54, no. 2, p. 23404, 2011.